Sulfonated polystyrene-modified mesoporous organosilicas for acid-catalyzed processes

Gabriel Morales*, Rafael van Grieken, Antonio Martín and Fernando Martínez

Department of Chemical and Environmental Technology. ESCET. Universidad Rey Juan Carlos. C/ Tulipán s/n, 28933, Móstoles (Madrid), Spain.

Published on: Chemical Engineering Journal 161 (2010) 388-396

Doi: http://dx.doi.org/10.1016/j.cej.2010.01.035>

* To whom correspondence should be addressed

Tel: +34 91 488 80 91. Fax: +34 91 488 70 68

e-mail address: gabriel.morales@urjc.es

Abstract

Organically-modified mesoporous silica materials have been prepared by direct co-condensation of styrylethyltrimethoxysilane (STETMOS) and tetraethylorthosilicate (TEOS) in one-pot synthesis. The polimerizable nature of the styryl-containing precursor induces the formation of anchored polystyrene blocks on the silica surface, which are amenable to be functionalized with acid groups via sulfonation. The resultant organosulfonic-modified mesostructured silica materials exhibit hexagonal long-range mesoscopic arrangement with extended surface areas and narrow mean pore size distributions. Upon sulfonation a high number of sulfonic acid sites have been introduced on the silica-anchored polystyrene-type organic moieties, thus providing strong acid sites embedded in a hydrophobic micro-environment. The catalytic performance of these strongly acidic hydrophobic materials has been assessed and compared with commercial catalysts in three different acid-catalyzed reactions. Two of them are acid strength-demanding reactions such as acylation of anisole with acetic anhydride and Fries rearrangement of phenyl acetate. The third one, based on the esterification of oleic acid with *n*-butanol, is a catalytic test wherein the hydrophobic nature of the catalyst surface plays an essential role. As result of these catalytic tests, the sulfonated polystyrene-modified hybrid materials have been shown as versatile and highly active acid heterogeneous catalysts, especially in hydrophobicity-demanding systems.

Keywords: organosilica, mesoporous, polystyrene, esterification, oleic acid.

1. Introduction

The development of heterogeneous catalysts to replace homogeneous systems for the production of a wide range of chemicals is motivated by several potential advantages [1-2], such as easier separation of the catalyst from the reaction medium, greater catalyst stability, improved regenerability, and enhanced product selectivity. Likewise, the implementation of restrictive environmental legislations for traditional acid-catalyzed processes has provided an opportunity for new acid-solid catalysts to replace strong homogeneous acids [3-4].

Many novel heterogenized catalysts are based on silica supports, primarily because of their high surface areas and porosities, excellent stabilities (chemical and thermal), and facile functionalization with organic groups that can be robustly anchored to the surface. Mesostructured silica materials are particularly promising supports for active species, due to their very high surface areas (>800 m^2/g), large pore diameters (2-50 nm) for low diffusional constraints, and narrow pore size distributions with high active-site accessibility [5-7]. A number of recent studies have reported the incorporation of sulfonic-acid groups into mesostructured pore channels of SBA-type materials [8-15]. Furthermore, such acidity can be modified by including different organic moieties adjacent to the sulfonic-acid site, such as arene-sulfonic [13] or perfluorosulfonic groups [15-17], whose electron-withdrawing effect lead to higher acid strengths. Likewise, the maximization of the hydrophobicity [18] or hydrophilicity [15] surrounding the sulfonic-acid sites enables further applications of these materials. For example, sulfonic-acid functionalized mesoporous silicas have shown improved reaction properties over conventional homogeneous and commercial heterogeneous catalysts for a wide range of acid-catalyzed reactions, including esterification [12, 19-

21], condensation and addition [9, 22-23], etherification [24], rearrangement [25-27], Friedel-Crafts acylation [28], alkylation [27], and conversion of biorenewable molecules [29-30]. In the field of hybrid organic-inorganic mesoporous materials several strategies of synthesis have been proposed during the last few years. Among them, grafting techniques of trialkoxyorganosilanes onto surface silanol groups in mesostructured silicas have led to rather low loading of functional groups, thus not being adequate when an extensive covering of the surface is desired. In contrast, co-condensation of tetraalkoxysilanes ($(RO)_4Si$) with terminal trialkoxyorganosilanes ($(RO)_3SiR'$, where R' can be, in example, a styrene-containing organic moiety) in the presence of a structure-directing surfactant agent allows the incorporation of higher organic amounts within mesostructured silica.

Apart from the above functionalization with catalytically active sites, further organic modification can be introduced in this kind of mesoporous silicas in order to alter the surface hydrophobicity properties. In this context, an extensively studied approach for the synthesis of hybrid organic-inorganic materials is the preparation of PMOs (periodic mesoporous organosilicas) which follows a co-condensation protocol [31-34]. These materials have been shown to combine several advantageous aspects of both organic and inorganic species into mesoporous solids with mechanical, adsorption, and reaction properties that are different from either of the wholly organic or inorganic components. In addition, several works have reported improved catalytic performance of sulfonic-acid active sites supported on mesoporous organosilica in water-sensitive reactions [20,35-37]. The higher catalytic activity shown by these materials has been attributed to increased hydrophobicity near the sulfonic-acid moieties and enhanced diffusion of reactant and products within the hydrophobic mesopores**.** More recently, highly acidic perfluorosulfonic moieties have also been successfully incorporated into a PMO matrix

by reacting a previously synthesized PMO with 1,2,2-trifluoro-2-hydroxy-1-trifluoromethylethane sulfonic acid β-sultone [38], leading to an outstanding improvement in the alkylation of isobutene/1-butene as compared with SBA-15-supported perfluorosulfonic acid groups. Nevertheless, the stability of these perfluorosulfonic acid sites is critically compromised when polar solvents are used due to a significant leaching of the active species to the reaction medium [39]. Hydrophobic modification of the molecule comprising the acid moiety has also been contemplated as an alternative. In this context, a novel approach for the synthesis of sulfonic acid functionalized periodic mesoporous silicas via covalent attachment of 2-(3,4 epoxycyclohexyl) ethyl-trimethoxysilane or 3-glycidoxy-propyltrimethoxysilane followed by reaction with sulfite ions and mild hydrochloric acid, has led to materials with superior catalytic performance in esterification, acylation, and condensation reactions [40].

In the present work we present an alternative strategy for the preparation of organic-inorganic hybrid materials based on sulfonic acid-modified silicas. In this way, a co-condensation method has been used to incorporate a styryl-containing precursor with polimerizable nature in order to induce the formation of anchored oligo-styrene blocks covalently linked to the silica surface, wherein the incorporated phenyl rings are subsequently acid-functionalized via sulfonation. This allows the production of highly acid hybrid materials with hydrophobic pore surfaces. The incorporation of polystyrene on silica is widely known in literature [41] but it has been typically addressed to the preparation of silica particles completely covered by polymer for non-catalytic applications. To the best of our knowledge no previous attempts on grafting polimerizable styrenic functions within the pores of mesostructured silica have been made.

The acid strength-demanding property was assessed on the acylation of anisole with acetic anhydride and Fries rearrangement of phenyl acetate, whereas the role of surface hydrophobicity was evaluated by the esterification of oleic acid with *n*-butanol. Acylation of anisole has been commonly used as a catalytic test for the evaluation of a wide variety of acid solid catalysts [42-44]. Fries rearrangement of phenyl acetate yields valuable precursors in the pharmaceutical industry, e.g. methoxyacetophenones (MAP) for the synthesis of paracetamol [45] or 4-hydroxycoumarin and warfarin as key intermediates in the production of anticoagulant drugs [46]. On the other hand, the esterification of oleic acid has been traditionally used for the production of fatty acid esters as raw materials for emulsifiers in different applications such as food, polymer, lubricant, paint and ink additive, cosmetics, and perfume industries [47]. In the last years further interest has also been brought to their potential application as biofuels, specifically in the production of biodiesel [48-49]. Particularly, the reaction of oleic acid with *n*-butanol has been previously reported over highly acidic zirconium sulfate-based catalyst [50] or lipase enzymes [51].

2. Materials and Methods

2.1 Catalysts preparation and characterization

The organically-modified materials were prepared via co-condensation of tetraethyl-orthosilicate (TEOS, Aldrich) and styryl-containing organosilane (styrylethyl-trimethoxysilane; STETMOS, ABCR). A solution of tri-block copolymer Pluronic 123 (EO_{20} PO_{70} EO_{20}) in 1.9 M HCl was prepared at room temperature. The solution was then heated up to 40 ºC before adding the silica source (TEOS). After 1 hour of pre-hydrolysis time of TEOS, STETMOS was added at different STETMOS/TEOS molar ratios (10, 20, and 30%, corresponding to samples denoted as ST10, ST20, and ST30,

respectively). Hydrolysis and co-condensation of the precursor silanes around the templating surfactant micelles was allowed to proceed for 20 h at 40ºC with vigorous stirring. The solution was then aged under static conditions at 100ºC for 24 h. Solid materials were recovered by filtration and dried overnight at room temperature. Surfactant was removed by ethanol-washing under reflux followed by a mild thermal treatment (150ºC for 6 h). The resultant mesoporous organic-inorganic hybrid materials were successfully sulfonated following an adapted procedure described elsewhere [52], which uses a mixture of sulfuric acid and acetic anhydride as sulfonating agent. Scheme I depicts a graphical vision of the synthesis procedure.

Polystyrene-modified mesoporous hybrid materials were structurally characterized by means of X-ray powder diffraction, nitrogen adsorption-desorption, and Transmission Electron Microscopy (TEM). Nitrogen adsorption and desorption isotherms at 77 K were measured using a Micromeritics TRISTAR 3000 equipment. Data was analyzed using BJH and BET models, with total pore volume (Vp) being assigned at P/Po= 0.975. X-ray powder diffraction (XRD) patterns were acquired on a PHILIPS X`PERT diffractometer using Cu Kα radiation. Data was recorded from 0.6 to 5º (2θ) with a resolution of 0.02º. TEM microphotographs were acquired in a JEOL 2000 electron microscope operating at 200 kV.

Cationic-exchange capacities corresponding to the sulfonated mesostructured materials were determined potentiometrically using 2M NaCl (aq) as cationic-exchange agent, and subsequent dropwise addition of 0.01 M NaOH (aq) as titration agent. Sulfur and total organic contents were determined by means of elemental analysis (HCNS) in a Vario EL III apparatus and thermogravimetic analysis in a SDT 2960 simultaneous DSC-TGA from TA Instruments (5ºCmin^{-1} ramp up to 700ºC in air atmosphere). ^{29}Si

and ^{13}C CP solid-state MAS-NMR spectroscopy was used to characterize the environment of the silicon and carbon nuclei. All solid-state NMR experiments were conducted at room temperature under magnetic field strength of 9.4 T on a high-resolution Varian INFINITY PLUS 400 NMR spectrometer operating at frequencies of 100.4 MHz for ^{13}C and 79.5 MHz for ^{29}Si. Chemical shifts were referenced to the corresponding nuclei in tetramethylsilane. Solid-state single-pulse ^{29}Si MAS-NMR spectra were recorded using a $\pi/2$ pulse of 1.5 μs, a recycle delay of 20 s, and 3000 transients. Solid-state ^{13}C CP-MAS NMR spectra were recorded with a ^{1}H $\pi/2$ pulse of 1.7 μs, followed by a 2 ms CP contact time, a recycle delay of 2 s, and 3200 transients. Diffuse reflectance UV-vis spectra (DRUV-vis) were recorded using a Varian Cary-500 under ambient conditions within the wavelength range of 200-600 nm.

2.2 Commercial Catalysts

Nafion®/silica composite SAC-13 with resin content of approximately 13 wt % was supplied by Aldrich. Polystyrene-based cationic-exchange sulfonic acid resin Amberlyst-15 was also supplied by Aldrich.

2.3 Catalytic tests

In order to check the catalytic performance of the sulfonated polystyrene-based mesostructured materials, three different catalytic tests have been used: i) acylation of anisole, ii) Fries isomerization of phenyl acetate, and iii) esterification of oleic acid with *n*-butanol (see Scheme II).

All the catalytic tests were carried out in a teflon-lined stainless steel stirred autoclave equipped with a temperature controller and a pressure gauge. Reactants and catalysts were all charged at room temperature, the system was pressurised with nitrogen (4 bar)

to ensure liquid phase of reaction media, and finally the reaction medium was heated using a thermally-controlled oven up to the reaction temperature. Catalysts, either commercial or synthesized, were always loaded in powder form and stirring was fixed for all the experiments at 500 rpm in order to minimize mass transfer limitations. The operating conditions of each catalytic reaction were selected on the basis of previous results found in literature: i) acylation of anisole: temperature 150ºC, 80 anisole/catalyst mass ratio, 1:1 acetic anhydride/anisole molar ratio [28]; ii) Fries rearrangement: 150ºC, 60 phenyl acetate/catalyst mass ratio, 3:1 phenyl acetate/phenol mass ratio [25]; and iii) esterification of oleic acid: 115ºC, 1:1.2 oleic acid/*n*-butanol molar ratio, 2 wt% catalyst relative to oleic acid [50]. The monitoring of the catalytic process was carried out by means of samples taken at selected reaction times and analyzed by GC (Varian 3900 chromatograph) using a CP-SIL 8 CB column (30m x 0.25 mm, DF=0.25) equipped with a FID detector, optimizing temperature programme and choice of internal standard for each assay. The catalytic activity in the acylation of anisole and the esterification of oleic acid was determined in terms of the conversion of initial reactants, anisole and oleic acid, respectively. For the Fries rearrangement test, catalytic results are presented in terms of yield toward acetophenones products (APs). Additionally, a specific activity parameter has also been calculated in order to evaluate the mmol of disappeared reactants or resultant products per mmol of acid site. The distribution of products was also estimated by normalization of measurable compounds.

In the case of oleic acid esterification the influence of the reaction temperature and oleic acid/*n*-butanol molar ratio were also studied by means of a factorial design of experiments based on a 3^2 model [53]. The three levels for each variable were: *X*, oleic acid to *n*-butanol molar ratio (1:1, 1:1.2, and 1:1.4) and *Y*, the reaction temperature

(100, 115 and 135ºC); whereas conversion of oleic acid (%) was selected as response factor (*Z*) for the evaluation of the catalytic performance.

3. Results and Discussion

3.1 Characterization of the synthesized hybrid materials

Table 1 summarises textural properties of the different polystyrene-modified mesoporous organosilicas as well as purely siliceous mesostructured SBA-15 [54] for comparison purposes. As it can be seen in Table 1, organically-modified samples display adequate textural parameters, below those of pure SBA-15 but still well within the mesoporous range. This data also reveals that an increase in STETMOS organosilane content is clearly accompanied by the decrease of BET surface area and pore volume. In addition, the increase of STETMOS results in the reduction of the mean pore size down to approximately 6 nm, which promotes the increase of wall thicknesses.

Figure 1A shows N_2 adsorption-desorption isotherms evidencing the mesoporous nature of the synthesised materials (type IV isotherms with well defined hysteresis loops), and a progressive reduction in the adsorbed nitrogen volume as the organic content increases. XRD patterns of the series of ST-hybrid materials, illustrated in Figure 1B, evidence the typical low-angle diffraction pattern of hexagonal *p*6mm symmetry. Structures with long-range mesoscopic ordering may thus be inferred. The increase of the organosilane content translates into less degree of organosilica framework ordering, which confirms the typical structural-distorting phenomena observed in functionalized mesostructured silicas with high organic contents. Nevertheless, even the sample with

the highest polystyrenic content -ST30- displays an acceptable mesoporosity accompanied by an appropriate ordering degree.

The hexagonal arrangement of mesostructured SBA-15-type materials has also been confirmed by transmission electronic microscopy. TEM images of ST10, ST20 and ST30 samples evidenced the presence of regular hexagonally-arranged mesoporous domains, although they are more clearly defined in the samples with lower organic contents. Thus, ST10 was almost undistinguishable from pure SBA-15, whereas ST30 clearly showed areas of mesoporosity with low or none mesoscopic ordering (images not shown). Figure 2 depicts selected transmission micrographs of ST20 sample, which seems to present the optimal properties in terms of both acceptable extended surface area with appreciable mesoscopic ordering and intermediate organic content. Interestingly, pore size measurements directly performed on these micrographs are in fair agreement with the values obtained by N_2 adsorption shown in Table 1.

The incorporation of the organic precursor and the nature of the grafted organic moieties have been assessed by means of solid-state MAS-NMR. A single-pulse method was used for the NMR analysis of ^{29}Si nuclei, enabling the direct quantification of the different silicon species. Thus, Figure 3 depicts the spectra corresponding to the synthesised materials, in which the different types of silicon environments are shown: Q^n = $Si(OSi)_n(OX)_{4-n}$, wherein n = 2-4 (Q^2 at -90 ppm, Q^3 at -100 ppm y Q^4 at -110 ppm), and T^m = $RSi(OSi)_m(OX)_{3-m}$, wherein m = 2-3 (T^3 at -65 ppm y T^2 at -57 ppm). T^m signals reveal the presence of organic moieties chemically attached to the silica structure via Si-C bonds, and hence can be utilized for the calculation of the actual organic incorporation. The resulting values, 0.11 for sample ST10, 0.18 for sample ST20, and 0.29 for sample ST30, are in fair agreement with those theoretically

established in the synthesis procedure, 0.10, 0.20, and 0.30, respectively. This fact indicates a high organic incorporation yield of the synthesis method.

Solid-state ^{13}C CP MAS NMR displays signals associated to aromatic –chemical shifts at 126-144 ppm– and alkyl –15-28 ppm– functions that confirms the presence of polystyrene-type organic moieties. Chemical shifts at 70-75 ppm also indicate the residual presence of remaining surfactant after the extraction process. Figure 4A shows the ^{13}C CP MAS NMR spectrum of ST20 sample as example of the series of ST hybrid materials.

The presence of the styryl terminal groups of the organosilane precursor provides the opportunity for the formation of accessible polystyrene-type organic moieties on the silica surface. This fact could be demonstrated by means of DR-UV-Vis and solid-state ^{13}C CP MAS-NMR spectroscopies. DR-UV-Vis spectra (Figure 4B) showed that the band at 280 nm, attributed to non-polymerised styrenic olefin as determined by the SBA-15 silica sample impregnated with non-polymerized STETMOS precursor, is modified in all the ST hybrid materials. This band was displaced to lower wavelengths (255 nm), which correspond to aromatic rings with no olefin nearby. Also, solid-state ^{13}C CP MAS-NMR evidences the absence of a signal at 113 ppm, which is assignable to the terminal carbon atom in the olefin moiety of the styrenic group (see Figure 4A). Thus, its disappearance would be indicative of its chemical transformation by polymerization.

Table 2 shows the parameters related to the acidic properties of the mesoporous hybrid materials after the sulfonation process. As shown in this table, acid-exchange capacities estimated by acid-base titration after cationic exchange ranged from 0.96 to 1.70 meq of H^+/g. These values are within, or even over, the typical range of sulfonic acid-modified

mesoporous silicas. It must be noted that the sulfonation yield increases with the organosilane content up to values corresponding to sulfonated ST20 sample (S-ST20), which exhibits the highest acid capacity (1.70 mmol H^+/g) and sulfur content (1.66 meq S/g). However, a higher organosilane loading –as in the case of S-ST30 sample– did not result in an increase of the acid capacity or the sulfur content. This is attributed to less available polystyrene-type moieties to be sulfonated as a result of the reduced surface area and pore volume by the distortion of the mesoscopic SBA-15 ordering (Table 1). Since the generation of sulfonated moieties would take place only on accessible phenyl rings within the pore system, the accessibility to the generated sulfonic acid sites does not seem to be significantly limited by the organic loading of the hybrid material. Additionally, acid properties corresponding to other commercial solid catalysts (Nafion SAC-13 and Amberlyst-15) have also been included for comparison purposes in the following catalytic tests.

3.2 Catalytic evaluation

Sulfonated polystyrene-based hybrid materials (S-ST) were used in different acid-catalyzed reactions for the assessment of their acid strength and surface hydrophobicity. Acylation of anisole using acetic anhydride as acylating agent and Fries rearrangement of phenyl acetate at fixed reaction conditions were used as highly acid strength-demanding tests. On the other hand, esterification of oleic acid with *n*-butanol has been used as assay for the evaluation of acid catalyst with enhanced hydrophobic properties.

3.2.1 Reaction test for acid strength

Acylation of anisole and Fries rearrangement of phenyl acetate have been previously used as catalytic test to compare the activity of acid heterogeneous catalysts,

establishing the presence of strong Brönsted acid sites as an indispensable requirement to obtain high catalytic performances. Thus, relatively weak acid sites such as those in alkylsulfonic acid-functionalized materials, e.g. propyl-SO_3H acid sites, have shown poor or null activities in these reactions [25,28]. In contrast, superacid catalysts (e.g. perfluorinated sulfonic acid catalysts such as Nafion acid resin and silica-supported Nafion catalysts, either on amorphous silica (SAC-13) or mesostructured SBA-15 silica [55], and heteropolyacids such as $H_3PW_{12}O_{40}$ [56]) have been highly active. In the case of the sulfonated materials herein presented, the covalent bonding of sulfonic acid groups to phenyl rings as a result of the sulfonation of polystyrene-type moieties should provide them with relatively high acid strength. This has also been previously observed in arenesulfonic acid-functionalized mesostructured silicas [25,28], which showed a higher acid strength than the equivalent propyl-sulfonic acid-modified silica, being this fact attributed to the enhancement of electron withdrawing effect on the SO_3H group due to the nearby aromatic ring. Table 3 shows the catalytic activities of the different sulfonated ST hybrid materials in the two acid-strength demanding reactions, including two commercial acid heterogeneous catalysts, Amberlyst-15 and SAC-13, as references.

Prominent anisole conversions were obtained over S-ST samples. Within the series of S-ST materials, the best anisole conversion was achieved for the S-ST-20 sulfonated-mesoporous hybrid material (over 18%). In terms of specific activity, the behaviour of S-ST-20 and S-ST-30 samples was similar despite their rather different textural properties (Table 1), which is attributed to their similar acid capacities. This fact seems to indicate the concentration of acid sites as the main factor affecting the catalytic activity, rather than structural and textural properties. When compared with the commercial acid catalysts, catalytic activity of S-ST-20 was slightly higher than that shown by SAC-13. Concerning Amberlyst-15, although this resin yielded the highest

conversion of anisole, S-ST-20 mesostructured material provided better results in terms of specific activity, indicating a higher activity of the sulfonic acid sites. For the Fries rearrangement reaction, the catalytic results of the series of S-ST materials indicate an increase of the total APs yield with the increase of the organosilane precursor. Interestingly, S-ST-30 did not show a decreased activity in comparison with S-ST-20 as it was observed for the acylation of anisole. However, regarding the commercial catalyst, the activity of the S-ST materials evidenced a similar behaviour than those shown by the anisole acylation. Thus, the activity of S-ST materials was higher than that shown by SAC-13, which confirms the remarkable acid strength of the sulfonated polystyrene-based materials. Commercial resin Amberlyst-15 displayed the highest yield due to its superior acid capacity. Nevertheless, the use of this type of polymeric ionic-exchange resins is usually limited by thermal stability, being 120ºC the recommended maximum operating temperature for Amberlyst-15. In terms of specific activity the trend also reverses and SAC-13 appears as the catalyst with the most active sites whereas Amberlyst-15 shows the lowest values. In terms of selectivity to the most interesting product (*p*-HAP), S-ST catalysts displayed slightly superior values. Note also that the formation of *p*-AXAP, by-product with the lowest added value, is reduced over S-ST catalysts as compared with the commercial ones. The explanation for this enhancement of selectivity might rely on the presence of a mesoporous framework that would somehow limit the formation of the bulkier *p*-AXAP, as compared to macroporous systems in SAC-13 and Amberlyst-15.

3.2.2 Reaction test for hydrophobicity

Catalyst S-ST-20 was selected as the most promising material of the S-ST series from the above characterization and catalytic results for this reaction test. Thus, Figure 5

compares the activity of S-ST-20 with the two commercial catalysts in the esterification of oleic acid with *n*-butanol, and evidences its superior catalytic activity. This fact can be attributed to an adequate combination of acid strength and hydrophobic surface of the sulfonated polystyrene-based silica materials, which allows an efficient conversion of oleic acid promoted by a fluid diffusion of reactants and products. Importantly, S-ST-20 catalyst displays a kinetic curve for oleic acid conversion that is clearly over that of Amberlyts-15 resin, with a considerably lower concentration of acid sites (1.7 vs. 4.8 $meqH^{+}{\cdot}g^{-1}$). On the other hand, the generation of water as co-product during the esterification serves to explain the lower activity of the more hydrophilic material, SAC-13. Water molecules, as reaction product, are generated on the sulfonic acid sites. When the microenvironment surrounding these sites is hydrophilic in nature a local accumulation of water molecules around the sulfonic acid sites can be expected. Obviously, this would impair the esterification process either in kinetics or thermodynamic terms. This is especially clear in the case of SAC-13, where the high acid strength of its perfluorinated sulfonic acid sites also makes them highly hydrophilic. Such an effect has been previously reported for a similar reaction, the etherification of vanillyl alcohol with 1-hexanol, carried out over sulfonic acid-modified mesoporous silica [57]. Indeed, the avidity of sulfonic acid sites for water molecules has also been demonstrated by means of 2D HETCOR NMR [58].

Additionally, the influence of two reaction variables such as oleic acid/*n*-butanol molar ratio and temperature was studied using S-ST-20 as catalyst by means of a factorial design of experiments. Reaction temperature range was selected on the basis of previous studies [50]. The range of molar ratio has been set between a *n*-butanol-rich mixture and equimolar ratio, considering oleic acid as limitative reagent. Assuming a second order polynomial equation and using a Levenberg-Marquard algorithm for non-linear

regression, equation [1] has been deduced, where *X* and *Y* represent molar ratio and reaction temperature, respectively. Figure 6 summarizes the results of the factorial design of experiments.

$$Z \text{ (oleic acid conversion, \%)} = 82.95 + 8.16 \cdot X + 8.43 \cdot Y - 4.39 \cdot Y^2 - 1.28 \cdot X^2 - 1.55 \cdot X \cdot Y \qquad [1]$$

The 3D graphical representation of equation [1] in Figure 6A evidences a remarkable enhancement of the conversion of oleic acid when both the reaction temperature and the relative amount of *n*-butanol are increased. Thus, optimal reaction conditions in the studied range were 130 ºC and oleic acid/*n*-butanol molar ratio 1/1.4, which led to a conversion value over 92%. Concerning equation [1] coefficients, the presence of quadratic terms are responsible of a certain curvature of the response surface and allowed a better fitting of the mathematical equation to the experimental results. Coefficients terms related to the reaction temperature (*Y*) and oleic acid/*n*-butanol molar ratio (*X*) are quite close, which indicates a similar influence of both reaction variables on the conversion of oleic acid within the range under study. A graphical comparison of experimental results of oleic acid conversion and mathematical model-predicted values is also shown in Figure 6B. The fair agreement between both data sets serves to demonstrate the goodness of the mathematical fitting. The results from three replicas performed in the reaction conditions of the central point (115 ºC, oleic acid/*n*-BuOH = 1/1.2) provided a standard deviation for oleic acid conversion, which indicates that variations in conversion below 3% must be carefully discussed as they fall within the experimental error.

Finally, catalyst reusability has also been checked by means of two consecutive catalytic runs using the above-optimized reaction conditions. Catalyst reutilization was performed without any regeneration or washing treatment thereof. The resultant activity

in the second consecutive run adequately reproduced the conversion rate of the first run, indicating a promising reusability of the catalyst S-ST-20 in the esterification of oleic acid with n-butanol.

4. Conclusions

Polystyrene-modified mesoporous organosilicas synthesized by co-condensation using a styryl-containing organosilane precursor have allowed a valuable incorporation of polystyrenic moieties on a mesostructured silica surface. These hybrid materials have displayed good mesoscopic ordering and relatively high surface areas, in combination with a high content of organic moieties, which can be readily acid-functionalized by direct sulfonation of the phenyl rings. These sulfonated catalysts have been applied to rather different acid-catalyzed reaction tests such as acylation of anisole, Fries rearrangement of phenyl acetate, and esterification of oleic acid, aiming to asses their catalytic properties in terms of both acid strength and surface hydrophobicity. Comparing the results with commercial SAC-13 and Amberlyst-15 catalysts, the convenience of combining an appropriate surface hydrophobicity and strong Brönsted acid sites has been demonstrated.

Acknowledgements

The financial support by Ministerio de Educación y Ciencia through the Project CTQ2005-02375 is gratefully acknowledged. Antonio Martín thanks the Ministerio de Educación y Ciencia for the grant FPI (BES-2006-13357).

References

[1] T. Okuhara, Water-Tolerant Solid Acid Catalysts, Chem. Rev. 102 (2002) 3641-3666.

[2] J. H. Clark, D. J. Macquarrie, Handbook of Green Chemistry and Technology, Blackwell, Oxford (2002).

[3] M. A. Harmer, W.E. Farneth, Q. Sun, Towards the Sulfuric Acid of Solids**,** Adv. Mater. 10 (1998) 1255-1257.

[4] K. Wilson, J.H. Clark, Pure, Solid acids and their use as environmentally friendly catalysts in organic synthesis, Appl. Chem. 72 (2000) 1313-1319.

[5] A. Vinu, K. Z. Hossain, K. Ariga, Recent Advances in Functionalization of Mesoporous Silica, J. Nanosci. Nanotechnol. 5 (2005) 347-375.

[6] G. Oye, J. Sjoblom, M. Stocker, Synthesis, characterization and potential applications of new materials in the mesoporous range, Adv. Colloid Interface Sci. 89-90 (2001) 439-466.

[7] A. Corma, From Microporous to Mesoporous Molecular Sieve Materials and Their Use in Catalysis, Chem. Rev. 97 (1997) 2373-2420.

[8] W. Van Rhijn, D. De Vos, W. Bossaert, J. Bullen, B. Wouters, P. Grobet, P. A. Jacobs, Sulfonic acid bearing mesoporous materials as catalysts in furan and polyol derivatization, Stud. Surf. Sci. Catal. 117 (1998) 183.

[9] W. M. Van Rhijn, D.E. De Vos, B.F. Sels, W. D. Bossaert, P.A. Jacobs, Sulfonic acid functionalised ordered mesoporous materials as catalysts for condensation and esterification reactions**,** Chem. Commun. (1998) 317-318.

[10] M.H. Lim, C. F. Blanford, A. Stein, Synthesis of Ordered Microporous Silicates with Organosulfur Surface Groups and Their Applications as Solid Acid Catalysts, Chem. Mater. 10 (1998) 467-470.

[11] D. Margolese, J.A. Melero, S.C. Christiansen, B. F. Chmelka, G. D. Stucky, Direct Syntheses of Ordered SBA-15 Mesoporous Silica Containing Sulfonic Acid Groups, Chem. Mater. 12 (2000) 2448-2459.

[12] I. Díaz, F. Mohino, J. Pérez-Pariente, E. Sastre, Synthesis, characterization and catalytic activity of MCM-41-type mesoporous silicas functionalized with sulfonic acid, Appl. Catal. A: Gen. 205 (2001) 19-30.

[13] J. A. Melero, G. D. Stucky, R. van Grieken, G. Morales, Direct syntheses of ordered SBA-15 mesoporous materials containing arenesulfonic acid groups**,** J. Mater. Chem. 12 (2002) 1664-1670.

[14] J. A. Melero, R. van Grieken, G. Morales, Advances in the Synthesis and Catalytic Applications of Organosulfonic-Functionalized Mesostructured Materials, Chem. Rev. 106 (2006) 3790-3812.

[15] G.L. Athens, Y. Ein-Eli, B.F. Chmelka, Acid-Functionalized Mesostructured Aluminosilica for Hydrophilic Proton Conduction Membranes, Adv. Mater.19 (2007) 2580-2587.

[16] M. Alvaro, A. Corma, D. Das, V. Fornés, H. García, Single-step preparation and catalytic activity of mesoporous MCM-41 and SBA-15 silicas functionalized with perfluoroalkylsulfonic acid groups analogous to Nafion®**,** Chem. Commun. (2004) 956-957.

[17] D. J. Macquarrie, S. J. Tavener, M. A. Harmer, Novel mesoporous silica–perfluorosulfonic acid hybrids as strong heterogeneous Brønsted catalysts, Chem. Commun. (2005) 2363-2365.

[18] I. Díaz, C. Márquez-Alvárez, F. Mohino, J. Pérez-Pariente, E. Sastre, Combined Alkyl and Sulfonic Acid Functionalization of MCM-41-Type Silica: Part 1. Synthesis and Characterization, J. Catal. 193 (2000) 283-294.

[19] W.D. Bossaert, D. E. De Vos, W.M. Van Rhijn, J. Bullen, P.J. Grobet, P.A. Jacobs, Mesoporous Sulfonic Acids as Selective Heterogeneous Catalysts for the Synthesis of Monoglycerides, J. Catal. 182 (1999) 156-164.

[20] I. Díaz, C. Márquez-Alvárez, F. Mohino, J. Pérez-Pariente, E. Sastre, Combined Alkyl and Sulfonic Acid Functionalization of MCM-41-Type Silica: Part 2. Esterification of Glycerol with Fatty Acids, J. Catal. 193 (2000) 295-302.

[21] J. A. Melero, R. van Grieken, G. Morales, M. Paniagua, Acidic Mesoporous Silica for the Acetylation of Glycerol: Synthesis of Bioadditives to Petrol Fuel, Energy & Fuels 21 (2007) 1782-1791.

[22] D. Das, J. F. Lee, S. Cheng, Selective synthesis of Bisphenol-A over mesoporous MCM silica catalysts functionalized with sulfonic acid groups, J. Catal. 223 (2004) 152-160.

[23] K. Wilson, A. F. Fee, D. J. Macquarrie, J.H. Clark, Structure and reactivity of sol–gel sulphonic acid silicas, Appl. Catal. A: Gen. 228 (2002) 127-133.

[24] J. G. C. Shen, R. G. Herman, K. Klier, Sulfonic Acid-Functionalized Mesoporous Silica: Synthesis, Characterization, and Catalytic Reaction of Alcohol Coupling to Ethers, J. Phys. Chem. 106 (2002) 9975-9978.

[25] R. van Grieken, J. A. Melero, G. Morales, Fries rearrangement of phenyl acetate over sulfonic modified mesostructured SBA-15 materials, Appl. Catal. A: Gen. 289 (2005) 143-152.

[26] X. Wang, C. C. Che, S. Y. Chen, Y. Mou, S. Cheng, Arenesulfonic acid functionalized mesoporous silica as a novel acid catalyst for the liquid phase Beckmann

rearrangement of cyclohexanone oxime to ε-caprolactam Appl. Catal. 281 (2005) 47-54.

[27] B. Rác, A. Molnár, P. Forgo, M. Mohai, I. Bertoti, A comparative study of solid sulfonic acid catalysts based on various ordered mesoporous silica materials, J. Mol. Catal. A: Chem 244 (2006) 46-57.

[28] J. A. Melero, R. van Grieken, G. Morales, V. Nuño, Friedel Crafts acylation of aromatic compounds over arenesulfonic containing mesostructured SBA-15 materials, Catal. Commun. 5 (2004) 131-136.

[29] I.K. Mbaraka, B. H. Shanks, Conversion of oils and fats using advanced mesoporous heterogeneous catalysts, J. Am. Oil Chem. Soc. 83 (2006) 79-91.

[30] J. A. Bootsma, B. H. Shanks, Cellobiose hydrolysis using organic–inorganic hybrid mesoporous silica catalysts, Appl. Catal. A: Gen. 327 (2007) 44-51.

[31] Q. Yang, M. P. Kapoor, S. Inagaki, Sulfuric Acid-Functionalized Mesoporous Benzene−Silica with a Molecular-Scale Periodicity in the Walls, J. Am. Chem. Soc. 124 (2002) 9694-9695.

[32] M. P. Kapoor, Q. Yang, Y. Goto, S Inagaki, Biphenylene Bridged Bifunctional Hybrid Mesoporous Silsesquioxanes with Sulfonic Acid Functionalities and Crystalline Pore Walls, Chem. Lett. 32 (2003) 914-915.

[33] S. Hamoudi, S. Royer, S. Kaliaguine, Propyl- and arene-sulfonic acid functionalized periodic mesoporous organosilicas, Microporous Mesoporous Mater. 71 (2004) 17-25.

[34] X. Yuan, H. I. Lee, J. W. Kim, J. E. Yie, J. M. Kim, Periodic Mesoporous Organosilicas Functionalized with Sulfonic Acid Group. Synthesis and Alkylation of Phenol, Chem. Lett. 32 (2003) 650-651.

[35] Q. Yang, M.P. Kapoor, N. Shirokura, M. Ohashi, S. Inagaki, J. N. Kondo, K.J. Domen, Ethane-bridged hybrid mesoporous functionalized organosilicas with terminal sulfonic groups and their catalytic applications, J. Mater. Chem. 15 (2005) 666-673.

[36] B. Show, S. Hamoudi, M. H. Zahedi-Niaki, S. Kaliaguine, 1-Butanol etherification over sulfonated mesostructured silica and organo-silica, Microporous Mesoporous Mater. 79 (2005) 129-136.

[37] P.L. Dhepe, M. Ohashi, S. Inagaki, M. Ichikawa, A. Fukuoka, Hydrolysis of sugars catalyzed by water-tolerant sulfonated mesoporous silicas, Catal. Lett. 102 (3-4) (2005) 163-169.

[38] W. Shen, D. Dubé, S. Kaliaguine, Alkylation of isobutane/1-butene over periodic mesoporous organosilica functionalized with perfluoroalkylsulfonic acid group, Catal. Commun. 10 (2008) 291-294.

[39] G. Blanco-Brieva, J.M. Campos-Martin, M.P. de Frutos, J.L.G. Fierro, Preparation, Characterization, and Acidity Evaluation of Perfluorosulfonic Acid-Functionalized Silica Catalysts, Ind. Eng. Chem. Res. 47 (2008) 8005-8010.

[40] M.P. Kapoor, W. Fujii, Y. Kasama, M. Yanagi, H. Nanbu, L.R. Juneja, An alternate approach to the preparation of versatile sulfonic acid functionalized periodic mesoporous silicas with superior catalytic applications, J. Mater. Chem. 18 (2008) 4683-4691.

[41] H. Ma, L.L. Dai, Synthesis of polystyrene–silica composite particles via one-step nanoparticle-stabilized emulsion polymerization, J. Colloid Interface Sci. 333(2) (2009) 807-811.

[42] S.G. Wagholikar, P.S. Niphadkar, S. Mayadevi, S. Sivasanker, Acylation of anisole with long-chain carboxylic acids over wide pore zeolites, Appl. Catal. A: Gen. 317 (2007) 250-257.

[43] K.M. Parida, S. Mallick, G.C. Pradhan, Acylation of anisole over 12-heteropolyacid of tungsten and molybdenum promoted zirconia, J. Mol. Catal. A: Chem 297 (2009) 93-100.

[44] R. Selvin, H.-L. Hsu, T.-M. Her, Acylation of anisole with acetic anhydride using ZSM-5 catalysts: Effect of ZSM-5 particle size in the nanoscale range, Catal. Commun. 10(2) (2008) 169-172.

[45] J. Fritch, O. Fruchey, T. Horlenko, US Patent 4954652, Hoechst Celanese Corporation (1990).

[46] I. Uwaydah, M. Aslam, C. Brown, S. Fitzhenry, S., J. Mc Donough, US Patent 5696274 (1997).

[47] K. Mantri, K. Komura, Y. Sugi, $ZrOCl_2 \cdot 8H_2O$ catalysts for the esterification of long chain aliphatic carboxylic acids and alcohols. The enhancement of catalytic performance by supporting on ordered mesoporous silica, Green Chem. 7(9) (2005) 677-682.

[48] H.D. Hanh, N.T. Dong, K. Okitsu, R. Nishimura, Y. Maeda, Biodiesel production by esterification of oleic acid with short-chain alcohols under ultrasonic irradiation condition, Renew. Energy 34 (2009) 780-783.

[49] J.M. Marchetti, A.F. Errazu, Comparison of different heterogeneous catalysts and different alcohols for the esterification reaction of oleic acid, Fuel 87 (2008) 3477-3480.

[50] J.C. Juan, J. Zhang, M.A. Yarmo, Study of catalysts comprising zirconium sulfate supported on a mesoporous sieve HMS for esterification of fatty acids under solvent-free condition, Appl. Catal. A: Gen. 347 (2008) 133-141.

[51] G.N. Kraai, J.G.M. Winkleman, J.G. de Vries, H.J. Heeres, Kinetic studies on the Rhizomucor miehei lipase catalyzed esterification reaction of oleic acid with 1-butanol in a biphasic system, Biochem. Eng. J. 41 (2008) 87-94.

[52] H.S. Makowski, R.D. Lundberg, G.H. Singhal, US Patent 3870841 (1975).

[53] G.E.P. Box, W.G. Hunter, J.S. Hunter, Statistics for Experiments, an Introduction to Design, Data Analysis and Model Building; Wiley New York,(1978).

[54] D. Zhao, Q. Huo, J. Feng, B.F. Chmelka, G.D. Stucky, Nonionic Triblock and Star Diblock Copolymer and Oligomeric Surfactant Syntheses of Highly Ordered, Hydrothermally Stable, Mesoporous Silica Structures, J. Am. Chem. Soc. 120 (1998), 6024-6036.

[55] F. Martínez, G. Morales, A. Martín, R. van Grieken, Perfluorinated Nafion-modified SBA-15 materials for catalytic acylation of anisole, Appl. Catal. A: Gen. 347 (2008) 169-178.

[56] E.F. Kozhevnikova, E. Rafiee, I.V. Kozhevnikov, Fries rearrangement of aryl esters catalysed by heteropoly acid: catalyst regeneration and reuse, Appl. Catal. 260 (2004) 25-34.

[57] R. van Grieken, J.A. Melero, G. Morales, Etherification of benzyl alcohols with 1-hexanol over organosulfonic acid mesostructured materials, J. Mol. Catal. A: Chem. 256 (2006) 29-36.

[58] G. Morales, G. Athens, B.F. Chmelka, R. van Grieken, J.A. Melero, Aqueous-sensitive reaction sites in sulfonic acid-functionalized mesoporous silicas, J. Catal. 254 (2008) 205-217.

Tables

Table 1. Textural properties of mesoporous organic-silica composite materials.

Sample / Type	S_{BET} (m^2/g)	D_p [a] (Å)	V_t [a] (cm^3/g)	d_{100} [b] (Å)	Wall Thickness [c] (Å)
SBA-15 / Silica	675	89	1.06	95	21
ST10 / Hybrid (10%)	573	63	0.62	81	31
ST20 / Hybrid (20%)	374	59	0.44	83	36
ST30 / Hybrid (30%)	188	60	0.25	81	33

[a] Pore size and total pore volume calculated by BJH method. [b] d(100) spacing, measured from small-angle XRD. [c] Pore wall thickness calculated as the difference between lattice parameter (a_0) and mean pore diameter (D_p), being $a_o=2d(100)/\sqrt{3}$.

Table 2. Acid properties of the sulfonated-mesoporous hybrid materials.

Sample	Titration [a] (meq H^+/g)	S content [b] (meq S/g)	Accessibility [c] (%)
S-ST10	0.96	0.95	~100
S-ST20	1.70	1.66	~100
S-ST30	1.45	1.42	~100
SAC-13	0.14	0.16	87
Amberlyst-15	4.80	N.A.	N.A.

[a] Estimated by cationic-exchange in saturated NaCl solution followed by titration with 0.01M NaOH. [b] Sulfur content by elemental analysis. [c] Ratio between titration and sulfur content values. N.A.: non-available.

Table 3 Catalytic activity of the different materials in two acid strength-demanding reactions: acylation of anisole with acetic anhydride, and Fries rearrangement of phenyl acetate.

Catalyst	Acylation of anisole		Fries rearrangement of phenyl acetate				
	$X_{anisole}$ (%)	Specific activity [a]	Yield to APs [b] (%)	Specific activity [c]	Selectivity [d] (%)		
					p-HAP	*o*-HAP	*p*-AXAP
S-ST10	7.0	3.57	2.56	2.94	48	29	23
S-ST20	18.1	5.21	3.46	2.87	50	29	21
S-ST30	16.0	5.40	4.57	3.47	53	26	21
SAC-13	16.1	56.3	2.34	21.67	44	18	38
Amberlyst-15	34.8	3.68	9.24	2.12	42	32	26

[a] Specific activity as reacted mmol of anisole per mmol of acid site. [b] Total percent yield towards acetophenones (APs): *p*-HAP + *o*-HAP + *p*-AXAP. [c] Specific activity as produced mmol of APs per mmol of acid site. [d] Selectivities calculated excluding phenol due to its co-solvent role.

Figure Captions

Scheme I. Synthesis procedure for sulfonated polystyrene-modified mesoporous organosilicas.

Scheme II. Simplified reaction schemes for: A) acylation of anisole with acetic anhydride; B) Fries isomerization of phenyl acetate; and C) esterification of oleic acid with n-butanol.

Figure 1. A) Nitrogen adsorption-desorption isotherms at 77 K; and B) small-angle X-ray diffraction patterns for polystyrene-modified mesostructured organosilicas.

Figure 2. TEM images of cross and longitudinal sections of sample ST20.

Figure 3. ^{29}Si MAS-NMR spectra corresponding to the hybrid ST materials.

Figure 4. A) ^{13}C CP MAS-NMR spectrum corresponding to ST20 sample. B) DR-UV-VIS spectra of polystyrene-modified mesoporous organosilicas and SBA-15 impregnated with STETMOS.

Figure 5. Comparison of the catalytic activity of S-ST20, Amberlyst-15 and SAC-13 in the esterification of oleic acid with *n*-butanol. Reaction conditions: 115ºC; 1:1.2 oleic acid/*n*-butanol molar ratio; 2 wt.% catalyst referred to oleic acid mass.

Figure 6. A) 3D response surface of oleic acid conversion; and B) accuracy of predicted data vs. experimental results for the esterification of oleic acid with *n*-butanol. Reaction time: 2 h. Catalyst: S-ST-20 at 2 wt.% referred to oleic acid.

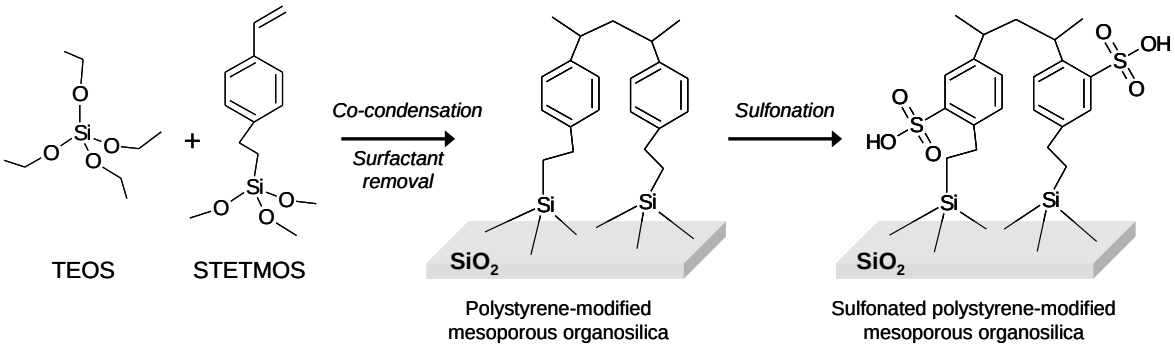

Scheme I

Gabriel Morales *et al*

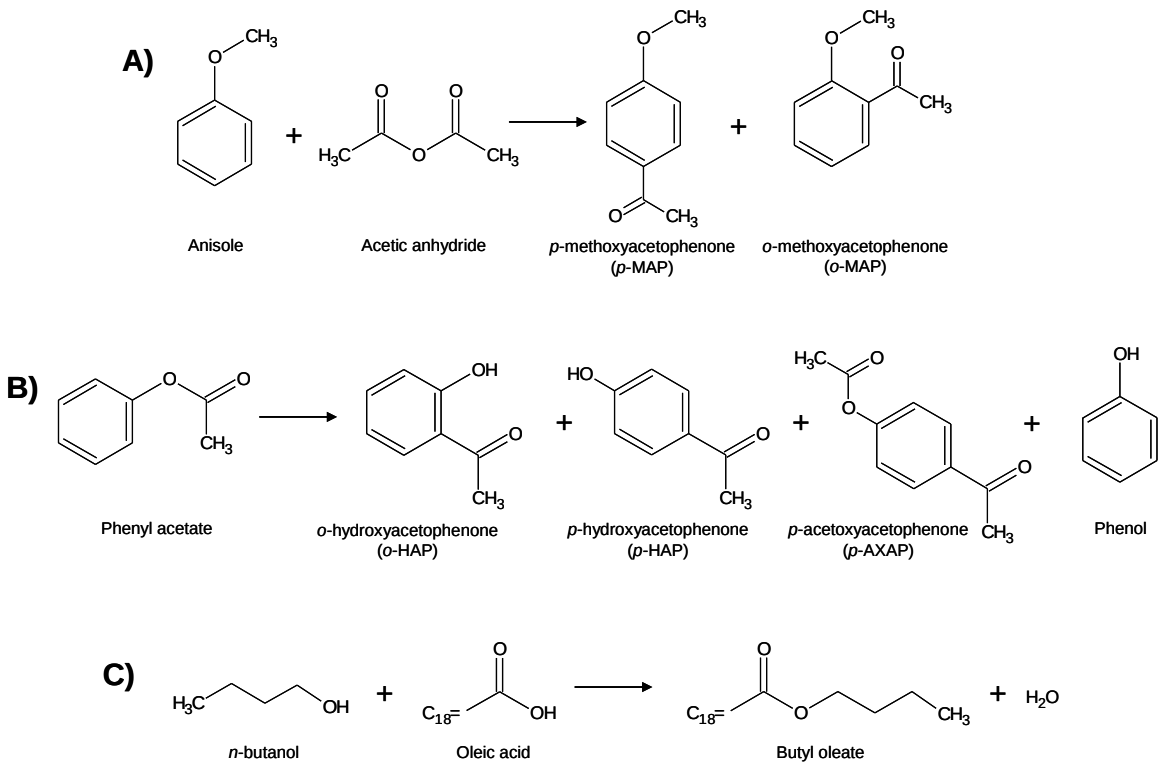

Scheme II

Gabriel Morales *et al*

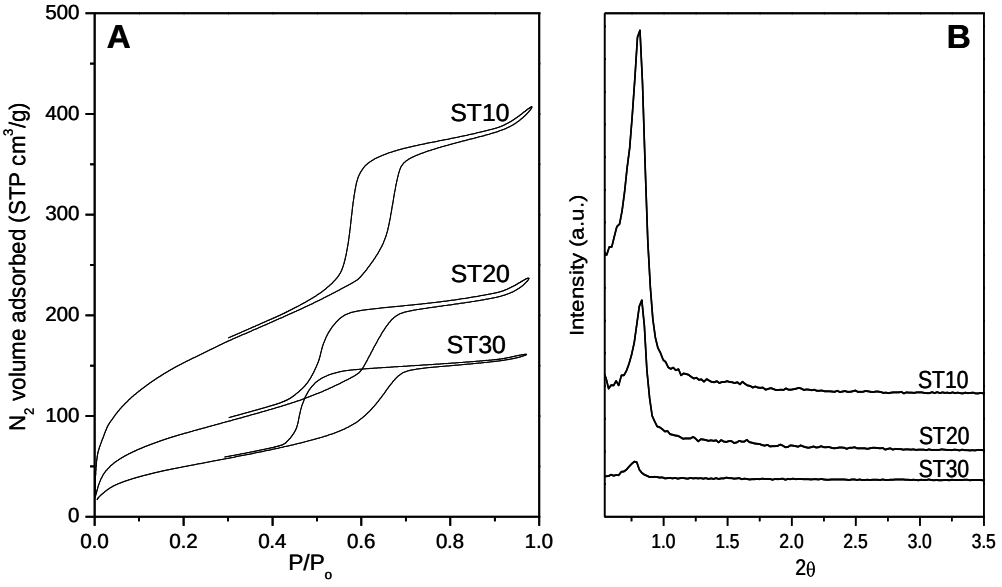

Figure 1

Gabriel Morales *et al*

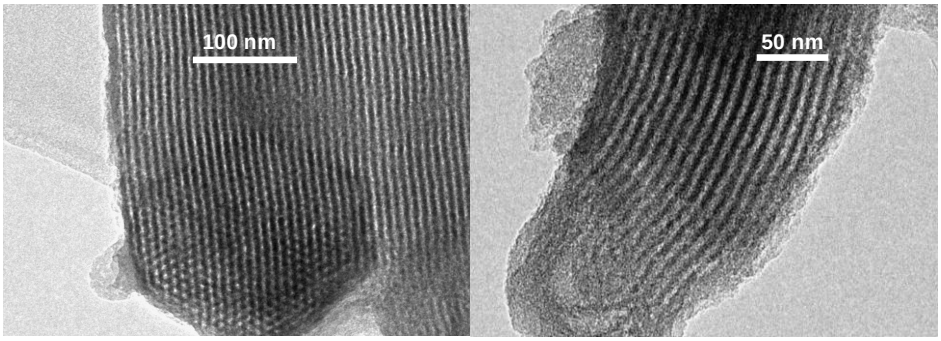

Figure 2

Gabriel Morales *et al*

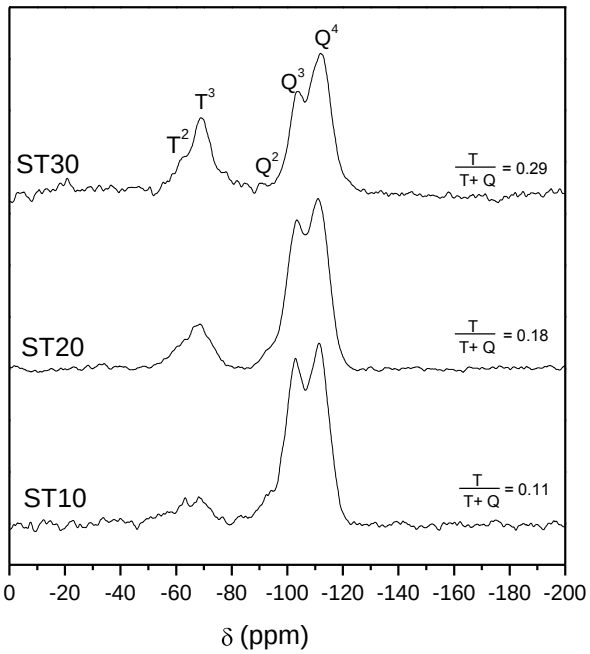

Figure 3

Gabriel Morales *et al*

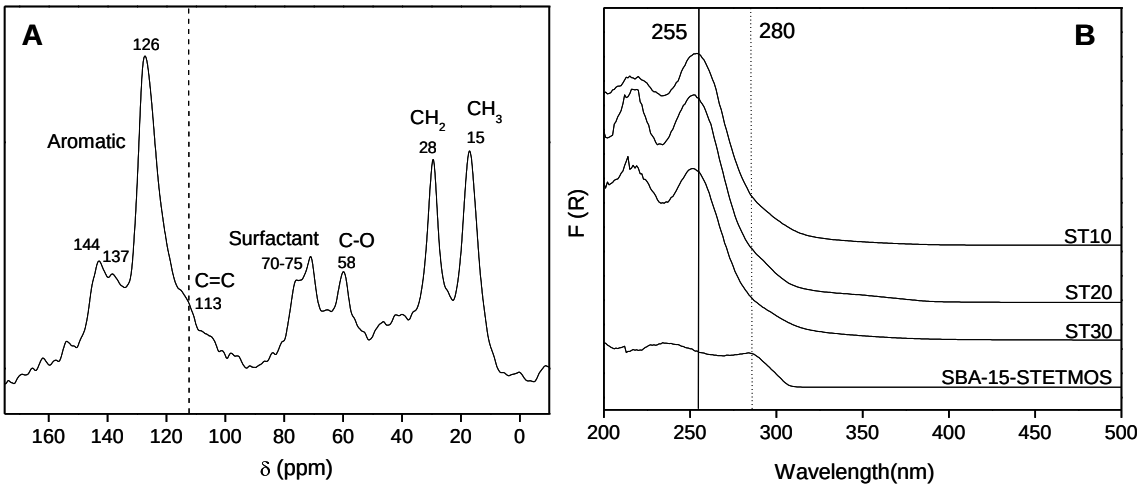

Figure 4

Gabriel Morales *et al*

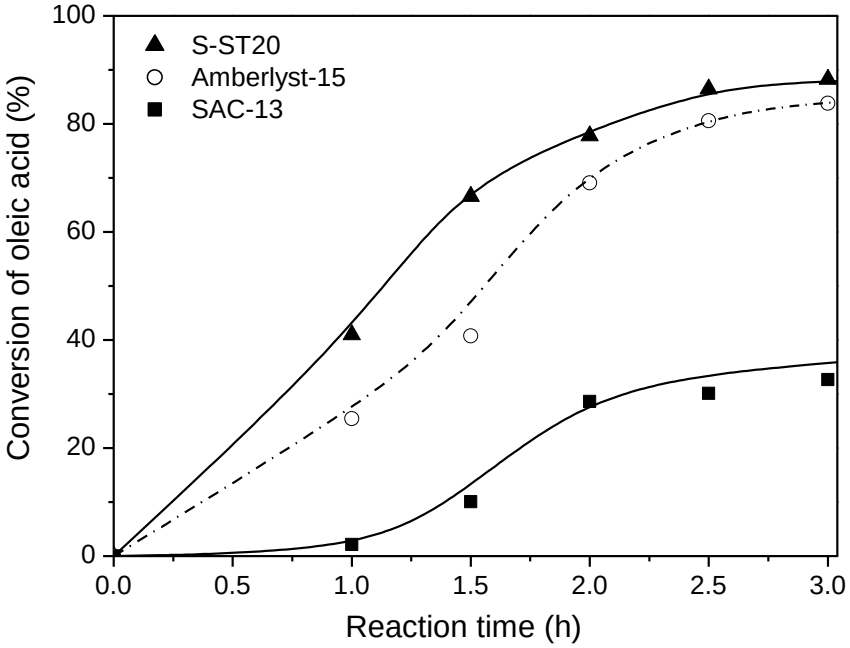

Figure 5

Gabriel Morales *et al*

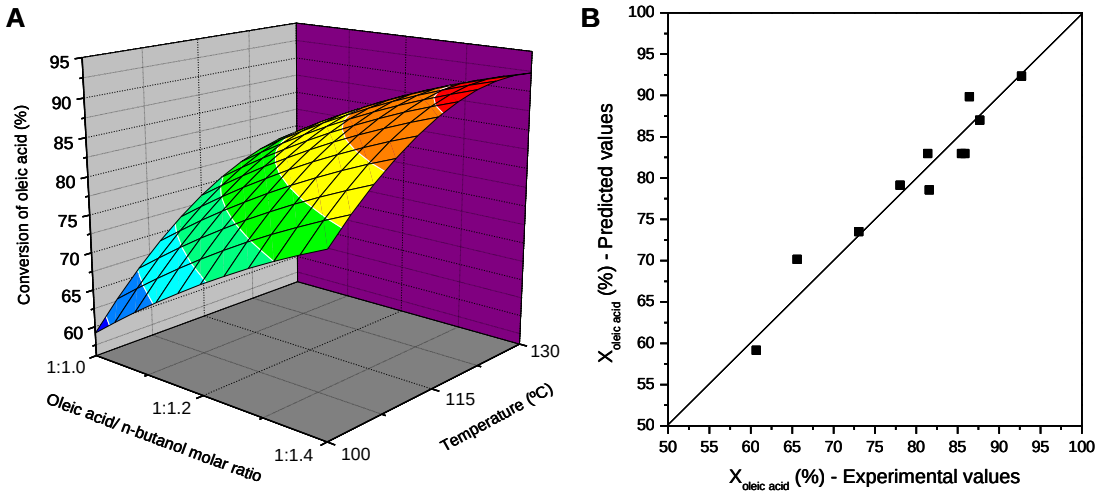

Figure 6

Gabriel Morales *et al*